Available online at www.sciencedirect.com
ScienceDirect
Acta Materialia 56 (2008) 1075–1083
Acta MATERIALIA
www.elsevier.com/locate/actamat

Size distribution and morphology of Cu_6Sn_5 scallops in wetting reaction between molten solder and copper

J.O. Suh [a,*], K.N. Tu [a], G.V. Lutsenko [b], A.M. Gusak [b]

[a] Department of Materials Science and Engineering, University of California at Los Angeles, Los Angeles, CA 90095-1595, USA
[b] Department of Theoretical Physics, Cherkasy National University, Cherkasy, Ukraine

Received 21 May 2007; received in revised form 2 November 2007; accepted 3 November 2007
Available online 18 January 2008

Abstract

During the reaction between molten solder and copper, ripening and growth of Cu_6Sn_5 scallops take place at the solder/metal interface. An experimental study on the morphology, size distribution and growth rate of Cu_6Sn_5 scallops was conducted. The measured size distributions of Cu_6Sn_5 as a function of time from top-view and cross-sectional view scanning electron microscopy images were in good agreement with the flux-driven ripening (FDR) theory. The FDR theory assumes a non-conservative ripening under a constant total interfacial area between the scallops and the solder, while the total volume of scallops increases with reaction time. The measured average radius of the scallops was proportional to the cube root of time. Comparing the experimental results and the theoretical model, the width of the liquid channel between scallops was calculated to be ~2.5 nm. Morphology of the scallop-type Cu_6Sn_5 was dependent to the composition of the solder. The scallop morphology became more faceted when the composition was further away from the eutectic composition. The Cu_6Sn_5 scallops with a shape close to hemispheric gave better agreement with FDR theory. The small difference between the experimental data and theory was explained by taking the noise factor into account. The modified FDR model showed even better agreement with the experimental data.

Keywords: Cu_6Sn_5; Solder wetting; Ripening

1. Introduction

The growth and ripening of scallop-type Cu_6Sn_5 in the wetting reaction between molten solder and Cu is a unique phenomenon of phase change. It was found that both growth and ripening of the scallops take place at the solder/metal interface at the same time [1]. Hence the ripening is a non-conservative ripening. Copper is constantly supplied through channels between the scallops to grow the scallops. The classic theory of the conservative ripening of precipitates by Lifshitz and Slyozov [2] and Wagner [3] (LSW theory) is not suitable for non-conservative ripening of scallops in solder joint formation. When molten solder wets a metal, the metal constantly diffuses through the narrow channels between intermetallic compound scallops to react with the tin in the molten solder and grows intermetallic compounds. Therefore, the system is an open system. This is the first major difference from classic LSW ripening, which assumes a closed system. Another major difference between the classic ripening and the current case of ripening of scallops in molten solder wetting reaction is distance among particles. The LSW theory assumes an infinitely dilute solution, which means the distance between precipitates is very large compared with the size of the particles. However, as in the top-view image of Cu_6Sn_5 scallops shown in Fig. 1, the scallops are almost in contact with each other, and their base is confined two-dimensionally at the interface between the solder and the metal. To have better physical model on formation and growth of intermetallic compound in reaction between molten solder and metal, an alternative kinetic model (flux-driven ripening (FDR) theory) was proposed [4].

* Corresponding author. Present address: Jet Propulsion Laboratory, Pasadena, CA, USA. Tel.: +1 818 354 574; fax: +1 818 393 6694.
E-mail address: Jong-ook.Suh@jpl.nasa.gov (J.O. Suh).

1359-6454/$34.00 © 2007 Acta Materialia Inc. Published by Elsevier Ltd. All rights reserved.
doi:10.1016/j.actamat.2007.11.009

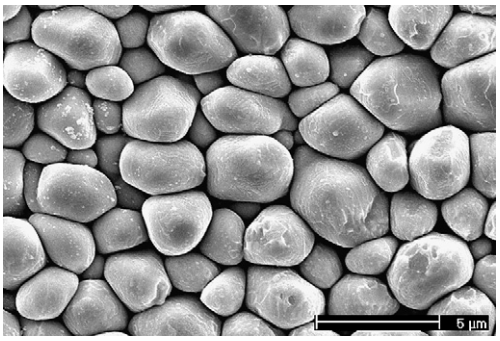

Fig. 1. Top-view image of Cu_6Sn_5 scallops formed by reaction between 50Sn50Pb solder and copper at 183.5 °C for 3 min.

The FDR model assumes, that the interfacial area between the intermetallic compound (IMC) and the molten solder is constant and that the shape of the scallops is hemispherical. As a result, the total interfacial area between the scallops and the molten solder becomes a constant, equal to twice the total interfacial area. However, the total volume of scallops increases with growth. In short, the ripening of the Cu_6Sn_5 in the FDR theory was assumed to be non-conservative ripening under a constant total surface area. The FDR theory was able to predict the scallop size distribution and rate of average size change according to the wetting reaction time. The size distribution curve is shown in Fig. 2, and the average radiu of the scallops $\langle r\rangle$ depends on time t, obeying the equation

$$\langle r\rangle = 0.913(kt)^{1/3} \tag{1}$$

The constant k in Eq. (1) is composed of several thermodynamic parameters. It is given as

$$k = \frac{9}{2}\frac{n}{n_i}\frac{D(C^b - C^e)\delta}{C_i} \tag{2}$$

where C_i is the Cu concentration in the scallop, C^e is the Cu concentration in the solder melt in stable equilibrium with a planar interface of Cu_6Sn_5, C^b is the quasi-equilibrium concentration of Cu in the vicinity of the Cu substrate, n is the atomic density in the molten solder, n_i is the atomic density in the scallop, D is the diffusivity of the Cu in the molten solder, and δ is the width of the channel between scallops.

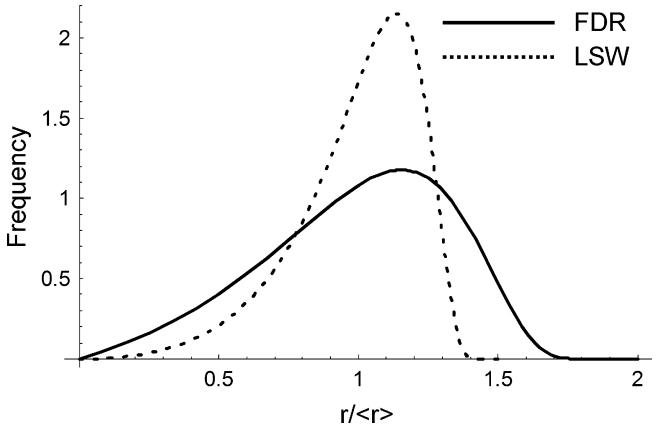

Fig. 2. Size distribution curve of FDR model, along with the curve of the LSW model.

This paper reports the experimentally measured size distribution of a large number of scallops as a function of wetting reaction time. A comparison with theoretical analysis is given. Furthermore, the morphology change of the scallops as a function of solder composition is presented.

2. Experimental

The effect of solder composition on the morphology of Cu_6Sn_5 scallops has been briefly mentioned in the literature [5]. The morphology of Cu_6Sn_5 scallops was found to be highly faceted when the solder was pure tin, and round when the solder was of eutectic composition. The morphology of the scallops may affect the kinetic path of their ripening, and the FDR theory assumes that the scallop shape is hemispherical. So the dependence of scallop morphology on solder composition and reaction temperature must be investigated systematically prior to the measurement of the size distribution and growth rate as functions of the reaction time.

To investigate the morphology of scallops in the SnPb/Cu reaction, samples with different solder compositions were prepared: pure Sn, 90Sn10Pb, 80Sn20Pb, 70Sn30Pb, 63Sn37Pb, 60Sn40Pb, 55Sn45Pb, 50Sn50Pb, 40Sn60Pb, 30Sn70Pb and 20Sn80Pb, in wt.%. Solder with a Pb concentration >90 wt.% Pb was not investigated, as Cu_3Sn will form instead of Cu_6Sn_5. Each alloy was prepared by mixing pure Sn (99.999%) and pure Pb (99.998%) in a quartz ampoule in a vacuum, and melting at 1150 °C for 1 h followed by quenching into ice water. To obtain a quenching rate high enough to produce homogenous alloys, only a small amount of alloy (~3 g) was prepared each time. The solder alloys were cut into small pieces (0.5 ± 0.1 mg) and melted in mildly activated flux (197 RMA) to form a spherical bead. Copper foil (99.999%) was cut into 1×1 cm square pieces 1 mm thick. Each Cu piece was mechanically polished down to colloidal silica to reduce the surface roughness, and ultrasonically cleaned with acetone, followed by methanol and DI water rinsing to remove organic contaminants on the surface. After removing the organics, the Cu foils were etched with 5% HNO_3+95% H_2O for 15 s to remove native oxide, and rinsed with DI water followed by drying with nitrogen gas. Then the Cu pieces were quickly immersed into the hot 197 RMA flux. The flux was used to improve the wettability of the solder. The solder bead was dropped onto the Cu foil immersed in the hot flux to form a solder cap. The solder bead melted and wetted the surface of the copper foil. To study the scallop morphology, samples were prepared at temperatures 20 °C above the melting temperature of each of the alloys. The temperature control was ±3 °C, and the reaction time was 2 min. To prepare samples to measure the size distribution of the scallops, the 55Sn45Pb solder was reacted with copper at 200 °C with

different reaction times of 30 s, 1 min, 2 min, 4 min and 8 min. In this study, the reaction time over 10 min was not investigated because vertical elongation of scallops is known to take place after 10 min [4], which can cause complications in data analysis. The reacted sample was taken out and quenched down to room temperature in acetone. To observe the size of the scallops, the unreacted solder covering the scallops was removed by mechanical polishing, followed by selective chemical etching. The selective etching was performed using 1 part nitric acid, 1 part acetic acid and 4 parts glycerol at 80 °C [6].

3. Results

3.1. Morphology of scallops of Cu_6Sn_5

Fig. 3 shows the change in scallop morphology as a function of different SnPb solder composition. The observed Cu_6Sn_5 scallop morphology is summarized in Table 1. When the Pb content of the SnPb solder was >70 wt.%, faceted scallops were observed all over the sample, along with some round scallops. When the Pb content of the solder was within the range from 60 wt.% to eutectic composition (34 wt.%), only round scallops were observed. When the Pb content was further decreased <30 wt.%, again faceted scallops were observed together with some round scallops. Finally, when the solder became pure tin, only faceted scallops were observed.

For the eutectic SnPb solder, some samples showed only round scallops. However, in other samples, large clusters of faceted scallops were observed at the center of the solder cap. This also took place when the solder composition was 60Sn40Pb. The authors postulate that the composition where the transition of scallop morphology takes place is close to the 63Sn37Pb and, when a small piece (0.5 mg) is taken out from a solder chunk (~3 g), inhomogeneity of the solder chunk may cause a change in the composition in the small piece. To determine the accurate scallop morphology of the eutectic SnPb solder, solders with 80Sn20Pb, 50Sn50Pb, 30Sn70Pb and eutectic (63Sn37Pb) composition were reacted with copper at 0.5 °C above eutectic temperature (183.5 °C). The temperature control was within ±1 °C. In this way, the solders underwent partial melting, and the composition of the liquidus phase became very close to the eutectic composition. At 183.5 °C, the morphology of the scallops had a round shape, regardless of solder composition. Thus the true morphology of Cu_6Sn_5 scallops when the SnPb solder composition is eutectic was obtained: it is smooth round scallop morphology.

Classical theories on the formation of a faceted or rounded liquid–solid interface cannot be directly applied to the current case of IMC/liquid solder interface, because the classical models assume a solid–liquid interface during solidification at equilibrium temperature [7,8], whereas in soldering a reaction takes place. However, the general idea in classic theories is that, if the interface is faceted, the adatoms at the surface of the solid phase tend to fill nearly all the available surface sites before advancing to the next atomic layer, resulting in an atomically flat interface with a small number of kink sites. If the crystal surface is round, the interface is more or less atomically rough, possessing a large number of kink sites for surface adatoms. To have round-shaped scallops, scallops should have many atomic steps and kinks at the surface. Since steps and kinks have many broken bonds, scallops can afford more kinks and steps at the surface when the broken bond energy is low. The broken bond energy is low when the IMC/solder interfacial energy is low. The IMC/solder interfacial energy is related to the wetting angle between the solder and the copper. When the molten solder wets the copper, the copper surface is replaced by the IMC/solder interface. Thus the IMC/solder interfacial energy is low when the solder/copper wetting angle is low, because the molten solder will prefer to spread out to increase the IMC/solder interfacial area. Liu [9] investigated the effect of SnPb solder composition on the wetting angle of molten SnPb on Cu and found the lowest wetting angle when solder composition was slightly higher in Pb than the eutectic composition (~55 wt.% Pb). This is in agreement with the finding shown in Table 1 that scallops had a round shape near the eutectic composition.

3.2. Size distribution and growth kinetics of Cu_6Sn_5

As the scallop morphology showed a dependence on solder composition, the solder with 55Sn45Pb composition was selected to ensure round morphology of the scallops for size distribution analysis. Fig. 4 is a log–log data plot of average radius vs time, to check the consistency with Eq. (1). The linear fitting was done by the linear regression method, and the growth exponent was obtained from the slope. Originally, the measured growth exponent was 0.35. The standard deviations of normalized particle size $r/\langle r\rangle$, where r is the radius of individual scallops, and $\langle r\rangle$ is the average radius of the scallops, showed a very small amount of variation with reaction time (~0.4). However, there was one data point with an exceptionally large value (0.670). This point was eliminated because it was considered to be unreliable. After removing the unreliable data point, the measured growth exponent became 0.33, and the measured value of k was $2.10 \times 10^{-14}\,\mathrm{cm^3\,s^{-1}}$. The average standard deviation was 0.423, which was larger than the theoretical value (0.331). This resembles the typical situation when the LSW theory is compared with experiments (LSW predicts standard deviations of 0.215, while experiment usually gives values ~0.3).

The average scallop height was also measured from cross-sectional SEM images, as shown in Fig. 5. The growth exponent was 0.35, and k was $2.40 \times 10^{-2}\,\mu\mathrm{m^3\,s^{-1}}$. The particle size distributions (PSD) are shown in Fig. 6. The theoretical distributions $f(r/\langle r\rangle)$ are normalized to $\int f(y)\mathrm{d}y = 1$, where $\langle r\rangle$ is the average radius. The heights of the histogram bars were also normalized for comparison

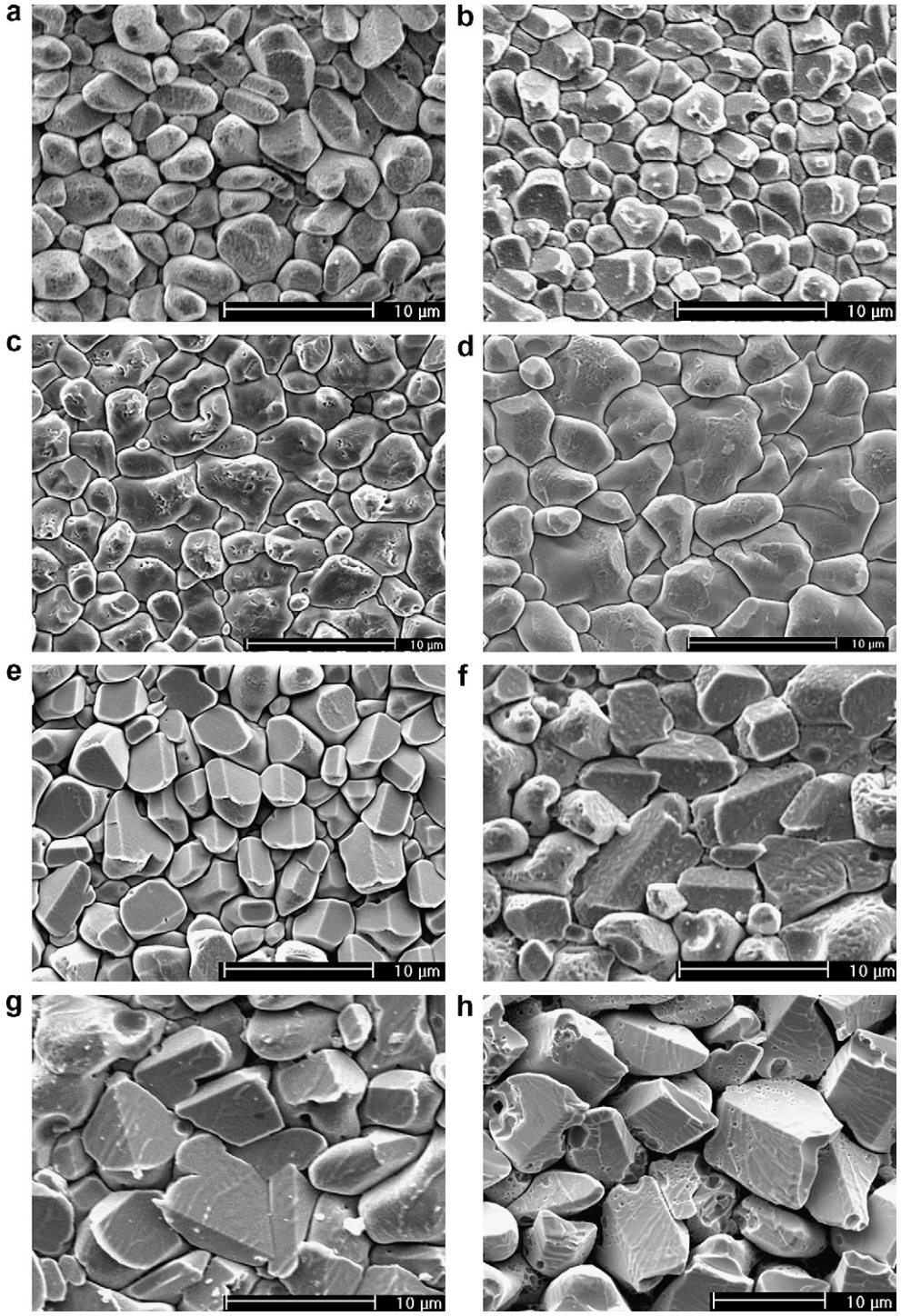

Fig. 3. SEM images of Cu_6Sn_5 IMC formed by wetting reaction with copper with solders: (a) 20Sn80Pb, (b) 30Sn70Pb, (c) 40Sn60Pb, (d) 50Sn50Pb, (e) 70Sn30Pb, (f) 80Sn20Pb, (g) 90Sn10Pb and (h) 100Sn.

Table 1
Summary of observed scallop morphology

Solder composition	20Sn80Pb	30Sn70Pb	40Sn60Pb	50Sn50Pb	55Sn45Pb	60Sn40Pb	63Sn37Pb	70Sn30Pb	80Sn20Pb	90Sn10Pb	100 Sn
Reaction temperature (°C)	295	275	255	235	200	200	200	210	225	240	250
Morphology	Facet	Facet	Round	Round	Round	Round	Round	Facet	Facet	Facet	Facet

Solders have reacted with copper for 2 min at 20 °C above their melting temperature.

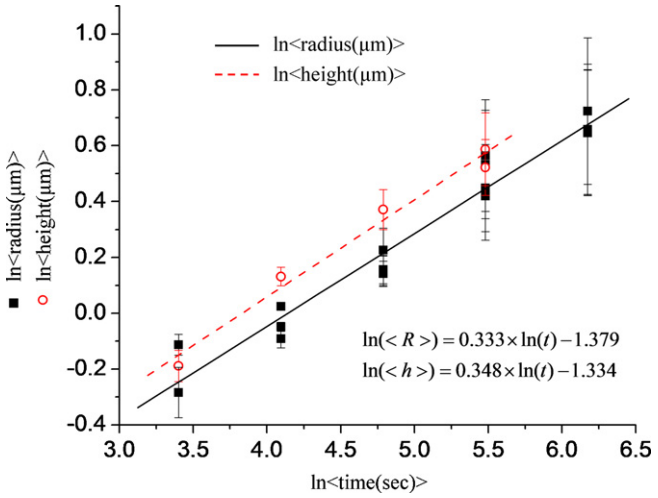

Fig. 4. Data plot of average radius vs time and height vs time Cu_6Sn_5 in reaction between 55Sn45Pb and copper at 200 °C.

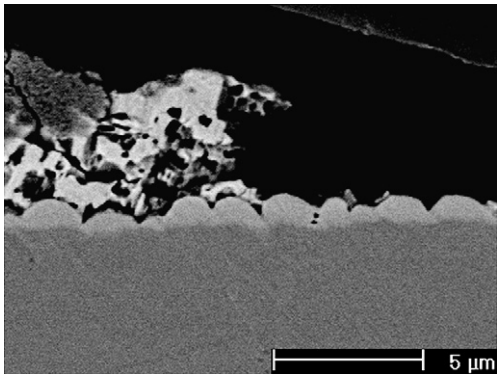

Fig. 5. Cross-sectional SEM image of Cu_6Sn_5 formed by reaction between 55Sn45Pb solder and copper at 200 °C for 30 s.

with the theoretical curve. Even though there was a small deviation, the experimental data showed fairly good agreement with the FDR model. The equation for the theoretical normalized curve of size distribution shown in Fig. 6a is given as [4]

$$g(u) = c\frac{u}{(2-u)^4}\exp\left(-\frac{4}{2-u}\right)$$

where u is the scaled particle size, defined as $u = r/\langle r\rangle$, and $g(u)$ is the probability density.

$$c = \left(\int_0^2 \frac{x}{(2-x)^4}\exp\left(-\frac{4}{2-x}\right)\mathrm{d}x\right)^{-1} = 0.0169$$

so that $g(u)$ is normalized to

$$\int_0^2 g(u)\mathrm{d}u = 1$$

The theoretical value of the standard deviation is

$$\sigma = \sqrt{\int_0^2 (u-1)^2 g(u)\mathrm{d}u} = 0.331$$

The theoretical value of skewness is

$$\frac{1}{\sigma^3}\int_0^2 (u-1)^3 g(u)\mathrm{d}u = -0.433$$

and the kurtosis is

$$\frac{1}{\sigma^4}\int_0^2 (u-1)^4 g(u)\mathrm{d}u - 3 = -0.403$$

Table 2 presents values of standard deviation, skewness and kurtosis, measured after different reflow times. Their average values were 0.423, −0.133 and −0.670, respectively.

Because cross-sectional SEM images were used to measure the height of the scallops, the number of scallops measured is much less than in the case of the radius distribution where the radius of scallops was measured from top-view images. Therefore, the height measurement data shown here is not statistically as reliable as the radius measurement, although the growth exponent of height vs time was also close to 1/3. The aspect ratio between height and radius remained almost constant. The average value of aspect ratio was 1.05.

4. Discussion

On the FDR model, the major differences from the LSW model are the constant surface area of growth and the existence of channels between scallops. The width of channel has not been measured directly, so the calculation based on experimental measurement is very important to the model. The constant k in Eq. (2) is composed of several thermodynamic parameters. To make a rough estimation of the channel width, one can take $C_i \approx 6/11$, $n/n_i \approx 1$, $D \approx 10^{-5}$ cm^2 s^{-1} and $C^b - C^e \approx 0.001$. $C^b - C^e$ was estimated by numerical thermodynamic calculation [4]. As $k = 2.10 \times 10^{-14}$ cm^3 s^{-1}, the channel width is calculated to be $\delta = 2.54$ nm, which means the channel width is in the nanometer scale. To validate the calculated channel width roughly, one can consider the upper and lower bounds of the channel width. The lower bound of the channel width is 0.5 nm, which is a typical grain boundary width in the solid state. If one takes a diffusivity of 10^{-8} cm^2 s^{-1}, which is on the order of the diffusivity of all fcc metals at their melting point, it should be the highest grain boundary diffusivity in the solid state, and the calculated channel width will represent an upper bound. Fig. 7 is a plot of diffusivity vs channel width. If one assumes a diffusivity of 10^{-8} cm^2 s^{-1}, the channel width is 2.54 μm. Obviously, this is an unreasonably large value because this value is comparable with the average diameter of the scallops. If one takes the channel width as 0.5 nm, the diffusivity is 5×10^{-5} cm^2 s^{-1}. Again, this is a high diffusivity for liquid, not for grain boundary. However, the calculated channel width needs to be confirmed experimentally. Wetting a molten SnPb solder on a bulk Cu_6Sn_5 surface will provide deep penetration of the

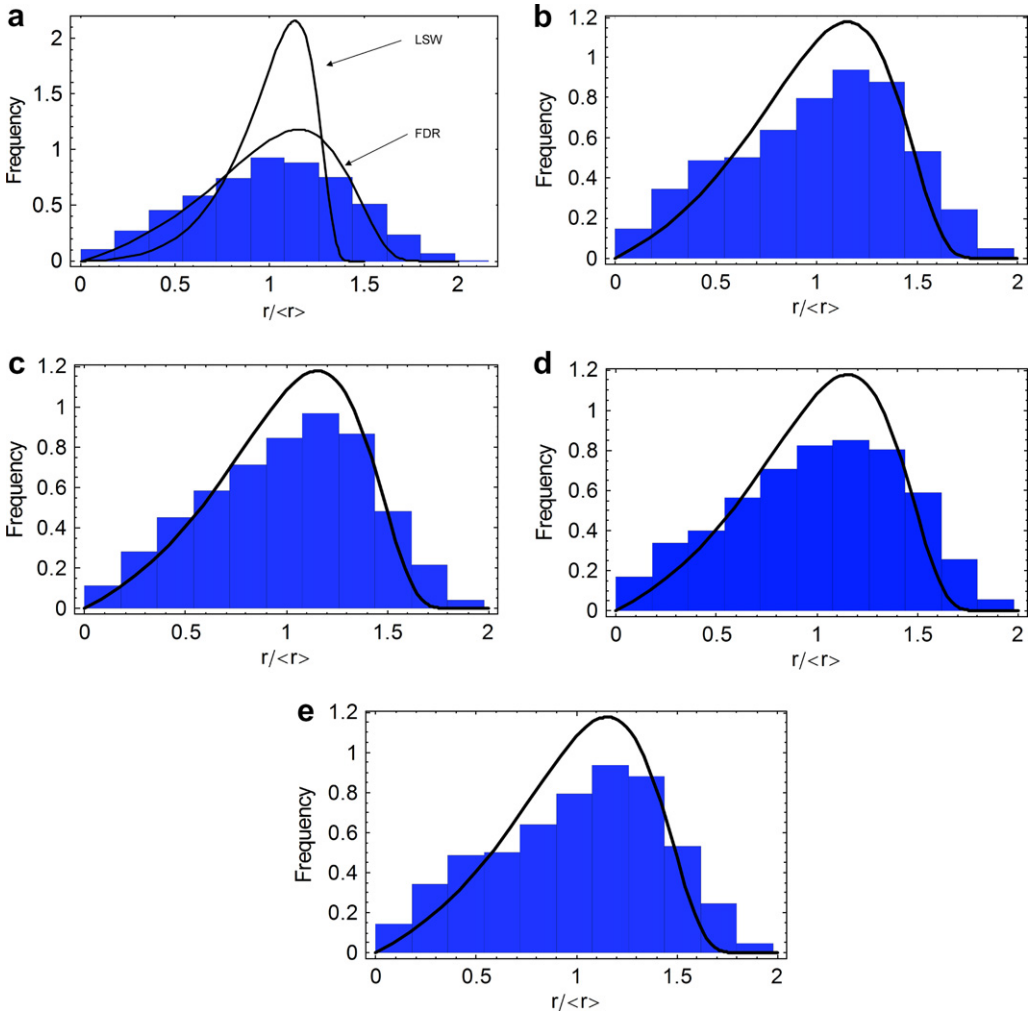

Fig. 6. Normalized PSD Cu_6Sn_5 scallops of (a) 30 s, (b) 1 min, (c) 2 min, (d) 4 min and (e) 8 min reflow. In (a), theoretical curves from LSW theory and FDR theory are shown for comparison.

Table 2
Statistical parameters of PSD of Cu_6Sn_5 in reaction between 55Sn45Pb and copper at 200 °C

Time (s)	Average radius $\langle r \rangle$ (μm)	Standard deviation σ, of $r/\langle r \rangle$	Skewness of $r/\langle r \rangle$	Kurtosis of $r/\langle r \rangle$
30	0.753	0.408	−0.126	−0.642
30	0.894	0.425	−0.096	−0.654
60	0.913	0.441	0.113	−0.575
60	1.025	0.415	−0.183	−0.628
60	0.953	0.406	−0.143	−0.662
120	1.164	0.428	−0.082	−0.560
120	1.169	0.410	−0.142	−0.572
120	1.253	0.434	−0.033	−0.743
120	1.152	0.399	−0.215	−0.618
240	1.566	0.455	−0.141	−0.796
240	1.760	0.433	−0.074	−0.712
240	1.522	0.417	−0.200	−0.667
240	1.704	0.419	−0.222	−0.718
480	1.933	0.428	−0.233	−0.740
480	1.908	0.417	−0.101	−0.630
480	1.910	0.418	−0.253	−0.735
480	2.062	0.434	−0.122	−0.741

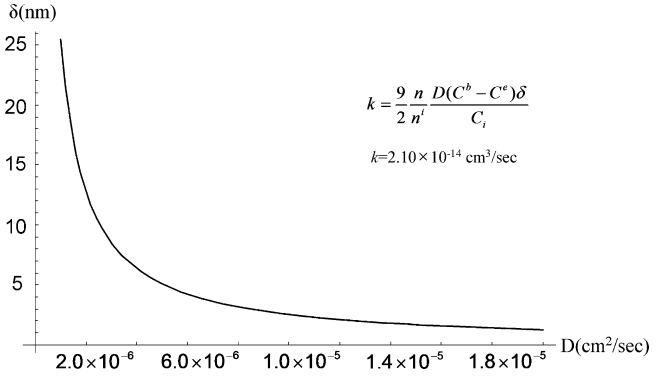

Fig. 7. Calculated relationship between diffusivity (D) of Cu through channel and channel width (δ).

solder into the grain boundaries of Cu_6Sn_5, and perhaps the exact width of the channel can be determined by transmission electron microscopy.

As the FDR assumes hemispherical scallops, it is of interest to see whether there is any change in ripening behavior when the scallop morphology deviates greatly from the hemispherical shape. Ghosh [10] investigated Ni_3Sn_4 formation by the reaction between various eutectic solders and Cu/Ni/Pd metallization. Ni_3Sn_4 scallops had an extremely faceted morphology, and their size distribution deviated greatly from the FDR theoretical curve. But their growth rate also followed $t^{1/3}$. Görlich et al. [11] investigated ripening of Cu_6Sn_5 when pure Sn reacted with Cu. The scallops had a faceted morphology, even though edges of scallops were more or less smoothened due to excessive chemical etching. The agreement with the theoretical model was not as good as in the current case of the round scallops, but was still in a relatively good agreement. The growth exponent was 0.34 for the scallop diameter and 0.40 for the height. This deviation from the theory can be examined in terms of geometric height-to-radius aspect ratio (height/(width/2)). In Görlich's work, average height-to-radius aspect ratio of scallops was ~0.71, while the average aspect ratio is 1.05 in the current study.

In the very early stage of the wetting reaction, nucleation of the scallops will have a greater effect on the size distribution. Thus, the PSD of short reaction time was expected to be less ideal. However, the size distribution of 30 s of reaction already showed very good agreement with the FDR theory. In addition, the standard deviations of PSD showed very little variation with reaction time (~0.4). This means that 30 s is enough time for ripening to be dominant over nucleation and growth and to achieve a stationary asymptotic state of distribution, which is stable in the reduced size scale $r/\langle r\rangle$.

5. Conclusion

In the wetting reaction between molten SnPb solder of varying composition and copper, the growth and ripening of Cu_6Sn_5 scallops obeys the FDR model of non-conservative ripening, assuming a constant interfacial area. The measured size distribution of the scallops is in good agreement with the FDR model, especially when the morphology of the scallops is close to hemispherical, as in the wetting reaction between eutectic SnPb and Cu. Minor deviations between the model and the experimental results can be reduced by taking noise into consideration, as is demonstrated in Appendix. The improved FDR model showed even better agreement with the experimental data.

Acknowledgement

The authors at UCLA would like to acknowledge the support from NSF contract DMR-0503726.

Appendix

The small difference between the measured statistical parameters and the theoretical values indicates that there is room for improvement of the FDR model. (This problem is also typical for PSD predicted by LSW theory for ripening in closed systems [12].) The origin of the deviation is considered to be from deviation of the local concentration of solute due to the large volume fraction of the scallops. The FDR theory was developed under mean field approximation, similar to the LSW theory. But if the new phase (precipitates or scallops) has a comparatively large volume fraction ($f > 0.02$) in standard Ostwald ripening, the deviations from the mean field caused by noise cannot be neglected [13]. The main origin of the noise is the deviation of local concentration (or chemical potential) from the mean field value in the parent phase. When a precipitate has a large volume fraction of closest neighbors, the closest neighbors will screen its diffusive interaction from more distant precipitates. Another reason for noise is the possible local fluctuations of diffusivity and surface tension. In the FDR theory, the volume fraction of scallops in the reaction zone is very large. The exact value of the volume fraction is difficult to tell. This is because the system is open near the scallops, and the scallops grow in the molten solder with a sharp concentration gradient in the scallop region. The copper atoms at the bottom of the scallops can be distributed only between the nearest neighboring scallops. In contrast, the copper atoms in the upper part of the solder bump can easily find their way to any scallop. It is assumed that the incoming Cu atoms have time and possibility to migrate all over the solder before attaching to some of the scallops. The volume fraction of scallops with average height h in the hemispherical solder bump with radius R can be roughly estimated as

$$f \approx \frac{\pi R^2 h}{\frac{2}{3}\pi R^3} \approx \frac{3}{2}\frac{h}{R} \tag{A1}$$

Even though this is a very rough estimation, the order of magnitude is correct. Take $h \approx 1.5\ \mu m$, which is about the average radius of scallops after 4 min reflow, and $R \approx 300\ \mu m$, which is about the radius of the solder bead. Then, one has $f \approx 0.0075$.

The noise level, the ratio of the average squared deviation of supersaturation in the vicinity of an arbitrary precipitate from the mean field value, is estimated as the equation below [13]:

$$v \equiv \frac{1}{\overline{\Delta}}\sqrt{\langle(\delta C)^2\rangle} \tag{A2}$$

where

$$\langle(\delta C)^2\rangle = \langle(\Delta - \overline{\Delta})^2\rangle \tag{A3}$$

where Δ is supersaturation in the vicinity of an arbitrary precipitate, and $\overline{\Delta}$ is the mean field value.

In a previous study [13], it was demonstrated that the noise level is approximately

$$v \approx f^{1/4} \cdot s \tag{A4}$$

where s is the standard deviation of PSD, which is equal to 0.215 in LSW and 0.33 in FDR. If one takes $s \approx 0.33$ and

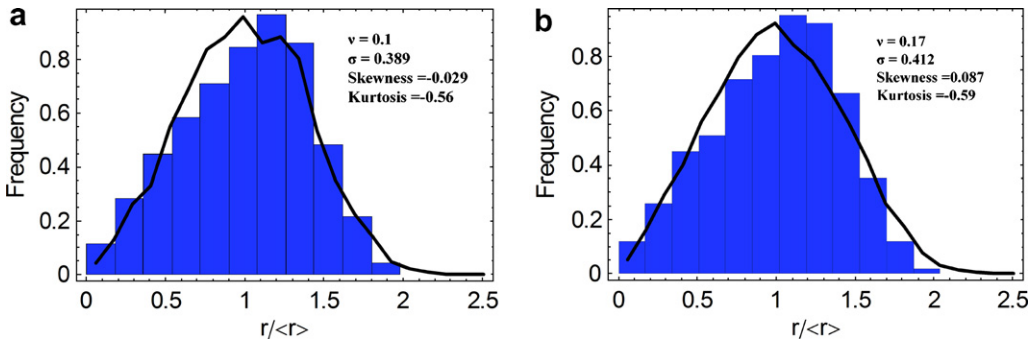

Fig. 8. Numerically calculated PSD (solid line) with noise of (a) $\nu = 0.1$ and (b) $\nu = 0.17$. Histogram in Fig. 6c is shown for comparison.

$f \approx 0.0075$ ($h \approx 1.5$ and $R \approx 300$ μm), $\nu \approx 0.1$. This can be considered as almost the lowest estimate of noise, because the short-range order effects and the possible scatter of channel widths were not considered. In the FDR model, the growth rate of the scallops is given as [4]

$$\frac{\mathrm{d}r_l}{\mathrm{d}t} = \frac{L}{nC_i}\left(\mu - \mu_\infty - \frac{\beta}{r_l}\right) \tag{A5}$$

where C_i is the quasi-equilibrium concentration of Cu in the vicinity of Cu_6Sn_5, μ is the average chemical potential of Cu in the reaction zone, μ_∞ is the equilibrium chemical potential for the flat interface, $\beta = 2\gamma\Omega$ (Ω is the molar volume, γ is the surface tension between the IMC and the liquid solder). The parameter L is similar to the Onsager coefficient and is determined self-consistently from the two constrains: constant surface and mass conservation [4].

Translating the noise of concentration into the noise of chemical potentials and adding the noise term, Eq. (A5) becomes

$$\frac{\mathrm{d}r_l}{\mathrm{d}t} = \frac{L}{n_i C_i}\left((\mu - \mu_\infty)\cdot(1+\varepsilon_l) - \frac{\beta}{r_l}\right) \tag{A6}$$

where ε_l is the relative noise of the chemical potential and the corresponding copper concentration, in the vicinity of the lth scallop. The ε_l is taken to be distributed according to Gaussian distribution with standard deviation, determined by the noise level ν.

As the total surface area of the particles is assumed to be constant in the FDR theory, one must substitute Eq. (A6) into the constraint of constant total surface $\mathrm{d}S/\mathrm{d}t = 0$

$$\begin{aligned}\frac{\mathrm{d}S}{\mathrm{d}t} &= 2\sum_l 2\pi r_l \frac{\mathrm{d}r_l}{\mathrm{d}t} \\ &= \frac{4\pi L}{n_i C_i}\left(\sum_l (\mu-\mu_\infty)(1+\varepsilon_l)r_l - N\beta\right) = 0\end{aligned} \tag{A7}$$

which gives

$$\mu - \mu_\infty = \frac{\beta}{\langle r\rangle + \langle \varepsilon r\rangle} \tag{A8}$$

In the FDR theory, it was assumed that all the incoming flux of copper is consumed by the growth in the total volume of the scallops. As a result, it was shown that [4]

$$\frac{3}{2}\frac{n}{n_i}\delta\frac{D\Delta C}{C_i} = \frac{3}{N}\sum_l r_l^2\frac{\mathrm{d}r_l}{\mathrm{d}t} \tag{A9}$$

Applying Eqs. (A6) and (A8) to (A9)

$$\begin{aligned}\frac{1}{2}\frac{n}{n_i}\delta\frac{D\Delta C}{C_i} &= \frac{1}{N}\sum_l r_l^2\frac{\mathrm{d}r_l}{\mathrm{d}t} \\ &= \frac{L}{n_i C_i N}\sum_l r_l^2\left(\frac{\beta(1+\varepsilon_l)}{\langle r\rangle + \langle \varepsilon r\rangle} - \frac{\beta}{r_l}\right) \\ &= \frac{L\beta}{n_i C_i}\left(\frac{\langle r^2\rangle + \langle \varepsilon r^2\rangle}{\langle r\rangle + \langle \varepsilon r\rangle} - \langle r\rangle\right) \\ &= \frac{L\beta}{n_i C_i}\frac{\langle r^2\rangle - \langle r\rangle^2 + \langle \varepsilon r^2\rangle - \langle r\rangle\langle \varepsilon r\rangle}{\langle r\rangle + \langle \varepsilon r\rangle}\end{aligned} \tag{A10}$$

Eq. (A10) immediately gives, together with Eqs. (A6) and (A8)

$$\frac{\mathrm{d}r_l}{\mathrm{d}t} = \frac{k}{9}\frac{(1+\varepsilon_l) - \frac{\langle r\rangle + \langle \varepsilon r\rangle}{r_l}}{\langle r^2\rangle - \langle r\rangle^2 + \langle r^2\varepsilon\rangle - \langle r\rangle\langle r\varepsilon\rangle} \tag{A11}$$

with

$$k = \frac{9}{2}\frac{n}{n_i}\frac{D\Delta C}{C_i}\delta \tag{A12}$$

So far, one can only treat this problem numerically.

A simple numerical method developed for LSW case was used for noise in the FDR case [13]. Taking into account that scallops are consumed one by one by their more successful competitors, one can numerically solve the set of N differential equations for squared radii

$$\frac{\mathrm{d}r_l^2}{\mathrm{d}t} = \frac{2k}{9}\frac{r_l(1+\varepsilon_l) - \langle r\rangle - \langle \varepsilon r\rangle}{\langle r^2\rangle - \langle r\rangle^2 + \langle r^2\varepsilon\rangle - \langle r\rangle\langle r\varepsilon\rangle} \tag{A13}$$

Fig. 8 presents size distributions for different noise levels obtained by the numerical method. The histogram in Fig. 6c is shown along with numerically calculated curves for comparison. The noise leads to broader, more symmetrical and less sharp distributions. The distribution should change with time owing to the noise, but the standard deviation tends to converge to some limit, depending on the noise level. If one takes $\nu = 0.1$, the standard deviation, skewness and kurtosis are 0.389, −0.029 and −0.56, respectively. If $\nu = 0.17$, they are 0.412, 0.087 and −0.59, which is closer to the experimental data.

References

[1] Kim HK, Tu KN. Phys Rev B 1996;53:16027–34.
[2] Lifshitz IM, Slyozov VV. J Phys Chem Solids 1961;19:35–50.
[3] Wagner CZ. Elektrochem 1961;65:581–91.
[4] Gusak AM, Tu KN. Phys Rev B 2002;66(11):115403.
[5] Tu KN, Gusak AM, Li M. J Appl Phys 2003;93(3):1335–53.
[6] ASM. Metals handbook, 9th ed., vol. 9. Materials Park, OH: ASM; 1985. p. 416.
[7] Jackson KA. Prog Solid State Chem 1967;4:53–80.
[8] Temkin DE. Molecular roughness of the crystal-melt boundary. In: Sirota NN, Gorskii FK, Varikash VM, editors. Crystallization processes. New York (NY): Consultants Bureau; 1966. p. 15–23.
[9] Liu CY, Tu KN. J Mater Res 1998;13:37–44.
[10] Ghosh G. J Appl Phys 2000;88:6887–96.
[11] Görlich J, Schmitz G, Tu KN. Appl Phys Lett 2005;86:053106.
[12] Ardell AJ. Precipitate coarsening in solids: modern theories, chronic disagreement with experiment. In: Lorimer GW, editor. Phase transformations'87. London: Institute of Metals; 1988. p. 485–94.
[13] Gusak AM, Lutsenko GV. Philos Mag 2005;85:1323–31.